HHS Public Access

Author manuscript

Circ Heart Fail. Author manuscript; available in PMC 2017 February 01.

Published in final edited form as:

Circ Heart Fail. 2016 February ; 9(2): e002206. doi:10.1161/CIRCHEARTFAILURE.115.002206.

Chronic Therapy with Elamipretide (MTP-131), a Novel Mitochondria-Targeting Peptide, Improves Left Ventricular and Mitochondrial Function in Dogs with Advanced Heart Failure

Hani N. Sabbah, PhD, FAHA, **Ramesh C. Gupta, PhD**, **Smita Kohli, MD**, **Mengjun Wang, MD**, **Souheila Hachem, BS**, and **Kefei Zhang, MD**

Department of Medicine, Division of Cardiovascular Medicine, Henry Ford Hospital, Detroit, Michigan

Abstract

Background—Elamipretide (MTP-131), a novel mitochondria-targeting peptide, was shown to reduce infarct size in animals with myocardial infarction and improve renal function in pigs with acute and chronic kidney injury. This study examined the effects of chronic therapy with elamipretide on left ventricular (LV) and mitochondrial (MITO) function in dogs with heart failure (HF).

Methods and Results—14 dogs with microembolization-induced HF were randomized to 3 months monotherapy with subcutaneous injections of elamipretide (0.5 mg/kg once daily, HF +ELA, n=7) or saline (Control, HF-CON, n=7). LV ejection fraction (EF), plasma n-terminal pro-brain natriuretic peptide (nt-pro BNP), tumor necrosis factor-alpha (TNF-α) and C-reactive protein (CRP) were measured before (pre-treatment) and 3 months after initiating therapy (post-treatment). MITO respiration, membrane potential (Δψm), maximum rate of ATP synthesis and ATP/ADP ratio were measured in isolated LV cardiomyocytes obtained at post-treatment. In HF-CON dogs, EF decreased at post-treatment compared to pre-treatment (29±1% vs. 31±2%); whereas in HF+ELA dogs, EF significantly increased at post-treatment compared to pre-treatment (36±2% vs. 30±2%, $p<0.05$). In HF-CON, nt-pro BNP increased by 88±120 pg/ml during follow-up but decreased significantly by 774±85 pg/ml in HF+ELA dogs ($p<0.001$). Treatment with elamipretide also normalized plasma TNF-α and CRP and restored MITO state-3 respiration, Δψm, rate of ATP synthesis and ATP/ADP ratio (ATP/ADP: 0.38±0.04 HF-CON vs. 1.16±0.15 HF+ELA, $p<0.001$).

Conclusions—Long-term therapy with elamipretide improves LV systolic function, normalizes plasma biomarkers and reverses MITO abnormalities in LV myocardium of dogs with advanced HF. The results support the development of elamipretide for the treatment of HF.

Correspondence to: Hani N. Sabbah, PhD, Director, Cardiovascular Research, Henry Ford Hospital, 2799 West Grand Boulevard, Detroit, Michigan 48202, Office Phone: (313) 916-7360, Office Fax: (313) 916-3001, hsabbah1@hfhs.org.

Disclosures

Dr. Sabbah has received research grants from Stealth Biotherapeutics, Inc. and is a consultant for Stealth Biotherapeutics. Drs. Gupta, Kohli, Wang and Zhang and Ms. Hachem have no conflict of interest disclosures.

Keywords

heart failure; mitochondria; ventricular function; cardiolipin; myocardial energetics

Impaired mitochondrial (MITO) energy metabolism plays a key pathogenic role in age-related degenerative disorders and is centrally involved in organ ischemia/reperfusion injury (1–4). Abnormalities of MITO structure and function exist in the failing heart of humans and experimental animals evidenced by hyperplasia, reduced organelle size, diminished rate of ATP synthesis (5–8) and increased formation of reactive oxygen species (ROS). These abnormalities include poor respiration, reduced membrane potential ($\Delta\psi m$) and opening of the permeability transition pore (mPTP) (5–8). Efforts to directly target MITO abnormalities to improve energy availability, limit oxidative stress and ultimately improve LV function in HF have received little attention due to an absence of safe pharmacologic agents that can effectively modify MITO function.

Elamipretide (Bendavia™, MTP-131) is a water-soluble tetrapeptide with structural motifs of natural and synthetic amino-acids (9). Elamipretide crosses the MITO outer membrane and localize to the inner membrane where it associate with cardiolipin (CL), a phospholipid exclusively expressed on the inner MITO membrane. Cardiolipin plays a central role in cristae formation, MITO fusion, mtDNA stability and segregation and in the function and organization of the respiratory complexes into supercomplexes for oxidative phosphorylation (10–14). Elamipretide has been shown to enhance ATP synthesis in multiple organs including heart, kidney, neurons and skeletal muscle (15–19). This study, examined the effects of long-term therapy with elamipretide on LV and MITO function in dogs with HF.

Methods

The canine model of intracoronary microembolization-induced chronic HF used in this study was previously described in detail (20). Fourteen healthy mongrel dogs, weighing between 20.8 and 25.7 kg, underwent serial intracoronary microembolizations performed 1 to 2 weeks apart, to produce HF. Embolizations were discontinued when LV ejection fraction (EF), determined angiographically, was ~30%. The study was approved by Henry Ford Health System Institutional Animal Care and Use Committee and conformed to the National Institute of Health “Guide and Care for Use of Laboratory Animals”. (NIH publication No. 85–23). Six weeks after the last microembolizations, HF dogs were randomized to 3 months therapy with subcutaneous injections of elamipretide (0.5 mg/kg once daily, n=7, HF+ELA) or vehicle (normal saline, once daily, n=7). Vehicle-treated HF dogs served as controls (HF-CON). Intravenous elamipretide has a half-life of 4 hours in dogs, is 100% renally excreted with 99% recovery in urine 24 hours after administration. Elamipretide’s peak plasma concentration is 325 ng/ml at 1 hour post dosing at 0.05 mg/kg. In all dogs, hemodynamic, ventriculographic, echocardiographic and Doppler measurements were made at baseline, before treatment (pre-treatment) and repeated 3 months after initiating treatment (post-treatment). For more details on the methods in this study, please see online Supplemental Materials.

To gain further insight into the mechanism of action of elamipretide, we also examined the acute effects of intravenous elamipretide on LV function. In this acute study, 13 HF dogs were randomized to a 2 hour infusion of elamipretide (0.05 mg/kg/hr, n=7) or to a 2 hour infusion of v/v of normal saline (Control, n=5).

Determination of Plasma Biomarkers and ROS

Plasma levels of interleukin-6 (IL-6), tumor necrosis factor alpha (TNFα), C-reactive protein (CRP) and n-terminal-pro brain natriuretic peptide (nt-proBNP) were determined in EDTA-plasma using the principle of the double antibody sandwich Enzyme-linked immunosorbent assay (ELISA) with commercially available kits (21). Total burden ROS in plasma was determined using the luminol-dependent chemiluminescence assay and expressed as relative luminescence units (RLU)/ml (22).

Histomorphometric Measurements in LV Tissue

After the final hemodynamic study, and while under general anesthesia, the dog's chest was opened and the heart rapidly removed and LV tissue prepared for histological and biochemical evaluation. The volume fraction of replacement fibrosis (VFRF) and interstitial fibrosis (VFIF), myocyte cross-sectional area (MCSA), a measure of cardiomyocyte hypertrophy, capillary density (CD), and oxygen diffusion distance (ODD) were assessed histomorphometrically as previously described (23, 24). LV tissue from 7 normal dogs was used for comparisons. Tissue sections were stained with Gomori trichrome to identify fibrous tissue. Cryostat sections stained with fluorescein-labeled peanut agglutinin were used to delineate cardiomyocytes border to measure MCSA and sections double stained with rhodamine-labeled Griffonia Simplicifolia lectin I (GSL-I) were used to measure CD and ODD, the latter defined as half the distance between 2 adjoining capillaries.

Determination of Mitochondrial Function

The following MITO function measures were assessed in freshly collagenase-isolated, digitonin-permeabilized cardiomyocytes: MITO state-3 respiration was measured using a Clark-type electrode (Strathklein Respirometer) (6). MITO membrane potential ($\Delta\psi m$) was measured using the commercially available JC-1 cationic fluorescent dye kit (Sigma, St. Louis, MO). This assay is an indicator of mitochondrial potential which, in presence and absence of valinomycin, exhibits potential-dependent accumulation in mitochondria, as indicated by a fluorescence emission shift from green (495ex/534em) to red (495ex/590em) (7). Mitochondrial permeability transition pore (mPTP) opening was assessed using calcein (7). The rate of calcein exit through mPTP was measured by recording the fluorescence signal every 2 min and calculated as a percent change from maximal fluorescence signal. Mitochondrial maximal rate of ATP Synthesis and the ratio ATP/ADP were determined using the ApoSENSOR™ ADP/ATP ratio bioluminescent assay kit (BioVision, Milpitas, CA) (7). This assay utilizes the enzyme luciferase to catalyze the formation of light from ATP and luciferin. The effects of an *in-vitro* 1 hour incubation of isolated cardiomyocytes from 3 untreated HF dogs with varying concentrations of elamipretide (0.0, 0.01, 0.1, 1.0 μM) on MITO state-3 respiration was also examined. ADP-stimulated respiration was determined in aliquots of 10 μl gravity settled cardiomyocytes.

Determination of Mitochondrial Complex I and IV Activities

The activity of MITO complex-I was assayed spectrophotometrically in MITO membrane fractions obtained from LV anterior wall (25). Complex-I activity was calculated as the rotenone-sensitive NADH:ubiquinone oxidoreductase activity and expressed as nmoles/min/mg protein. The activity of MITO complex-IV (cytochrome c oxidase) was determined polarographically in MITO membrane fractions (25) and expressed as nmoles molecular oxygen/min/mg protein.

Determination of Abundances of Key Subunits of Complex-I, II, III, IV and V

Abundance of key subunits of MITO complexes was determined by Western blotting using the Total OXYPHOS Antibody Cocktail ab110413 (abcam, Cambridge, MA) and bands quantified in densitometric units. The subunits were as follows: Complex-I subunit NDUFB8 (CI-NDUFB8); Complex-II succinate dehydrogenase subunit B (CII-SDHB); Complex-III subunit Core 2 (CIII-C2); Complex-IV subunit I (CIV-SI) and Complex-V ATP synthase subunit a (CV-S a).

Western Blotting and Measurements of Cardiolipin and ROS

Western blotting was used to quantify changes in LV tissue levels of specific MITO functions/dynamics and signaling proteins. Western blots were performed using primary antibodies and horse radish peroxidase-coupled secondary antibodies. Protein bands were visualized by chemiluminescence reagents (Thermo Scientific, Pittsburg, PA). Proteins included endothelial nitric oxide synthase (eNOS), inducible nitric oxide synthase (iNOS), peroxisome proliferator-activated receptor coactivator-1α (PGC-1α), cytosolic cytochrome c, active caspase 3, sarcoplasmic reticulum (SR) Ca^{2+}-ATPase (SERCA-2a) and β-actin as internal control. Protein bands were bands were quantified in du.

Total cardiolipin (CL) and $(18:2)_4$CL species were measured using electrospray ionization mass spectroscopy (26) and quantified in nmol/mg of non-collagen protein. Total CL and $(18:2)_4$CL were normalized to LV MITO protein levels and quantified as nmol CL/mg of MITO protein. Total ROS in LV tissue was determined using the luminol-dependent chemiluminescence assay and expressed in RLU/μg protein (22). In addition to total ROS, 4-hydroxynonenal (4-HNE), a natural bi-product of lipid peroxidation and capable of binding to proteins and forming stable adducts, was also measured using the commercially available Oxiselect HNE-His Adduct ELISA Kit (Biolabs, Inc., San Diego, CA).

Statistical Analysis

Within group comparisons of hemodynamic, ventriculographic, echocardiographic, Doppler and plasma biomarker measures were made using repeated measures analysis of variance (ANOVA) with alpha set at 0.05. If significance was attained, pairwise comparisons between baseline, pre-treatment and post-treatment measures were made using the Student-Neuman-Keuls test with $p<0.05$ considered significant. To assess treatment effect, the change (Δ) in each measure from pre-treatment to post-treatment within each study arm was calculated and the Δs compared between the two groups using a t-statistic for two means with $p\leq0.05$ considered significant. Histological and biochemical measures between normal, HF-CON and HF+BEN dogs were compared using one way ANOVA with alpha set at 0.05.

If significance was attained by ANOVA, pairwise comparisons were performed using the Student-Neuman-Kuels test with $p<0.05$ considered significant. All the data exhibited normal distributions and nonparametric testing led to similar results. Data are reported as mean ± standard error of the mean (SEM).

Results

Effects of Acute Intravenous Infusion of Elamipretide

Compared to intravenous saline, intravenous elamipretide had no effect on heart rate (HR), mean aortic pressure (mAoP) or systemic vascular resistance (SVR) (Fig. 1). Elamipretide had no effect on LV end-diastolic volume (EDV) but significantly decreased end-systolic volume (ESV) and significantly increased EF and stroke volume (SV) (Fig. 1).

Chronic Studies with Subcutaneous Elamipretide

Within Group Changes in Hemodynamics and Plasma Biomarkers— Hemodynamic, ventriculographic, echocardiographic, Doppler and plasma biomarker results are shown in Table 1. There were no significant differences between the 2 study groups in any measures obtained at baseline or at pre-treatment. In the HF-CON, HR, mAoP, LV end-diastolic pressure (EDP), SV, cardiac output (CO), cardiac index (CI), SVR, ratio of time-velocity integral of early mitral inflow velocity time-velocity integral during left atrial contraction (Ei/Ai), deceleration time of early mitral inflow velocity (DT), and LV circumferential end-diastolic wall stress (EDWS) did not change significantly over the course of 3 months of follow-up compared to pre-treatment values (Table 1). In the HF +ELA, HR, and mAoP were also not significantly changed during therapy. In this group, Ei/Ai and DT tended to increase but not significantly compared to pre-treatment (Table 1). Therapy with elamipretide significantly increased SV, CO, and CI and decreased EDP, SVR and EDWS.

In HF-CON, EDV and ESV tended to increase and EF tended to decrease at post-treatment compared to pre-treatment (Table 1). In HF+ELA, EDV was unchanged, ESV tended to decrease and EF increased significantly (Table 1). Plasma levels of nt-pro BNP, IL-6, TNF-α, CRP and ROS significantly increased in HF-CON compared to normal dogs. Treatment with elamipretide significantly reduced levels of all 5 biomarkers to near normal levels. In HF-CON, plasma levels of all 5 biomarkers remained markedly elevated throughout the treatment phase (Tables 1).

Between Groups Changes in Hemodynamics and Plasma Biomarkers (Treatment Effect)—Between-group comparisons of the change (Δ) between pre-treatment and post-treatment measurements are shown in Table 2 and Figure 1. Compared to HF-CON, long-term therapy with elamipretide had no effect on HR, mAoP, and SVR but tended to increase SV and decrease EDV and ESV. Treatment with elamipretide significantly increased EF, CO, CI and LV fractional area of shortening (FAS). Measures of LV diastolic function also tended to improve with elamipretide as evidenced by a decrease of EDP and EDWS and a trend for an increase in Ei/Ai and DT. Compared HF-CON,

elamipretide significantly decreased plasma levels of nt-pro BNP, IL-6, TNF-α, CRP and ROS to near normal levels (Fig. 2).

Histomorphometric Findings and Tissue ROS—Compared to normal dogs, HF-CON dogs showed significant increases in VFRF, VFIF, ODD and MCSA and a decrease in CD (Table 3). Elamipretide significantly reduced VFIF, ODD and MCSA and increased CD. The VFRF also tended to decrease but did not reach statistical significance. Total ROS in LV tissue was significantly higher in HF-CON compared to normal dogs and decreased to near normal in HF+ELA (Table 4). Levels of 4-HNE adducts were significantly higher in HF-CON compared to normal dogs and decreased to near normal in HF+ELA (Table 4).

Mitochondrial Function—Mitochondrial state-3 respiration, Δψm, maximum rate of ATP synthesis and ATP/ADP ratio were all decreased in HF-CON compared to normal dogs (Fig. 3). Treatment with elamipretide significantly increased all measures to near normal levels (Fig. 3). The rate of calcein exit was significantly slower in HF+ELA dogs compared to HF-CON (Fig. 3) indicative of reduced opening of the mPTP. Complex-I and complex-IV activities were significantly reduced in HF-CON compared to normal dogs (Fig. 4). Elamipretide significantly increased enzymatic activities of both complexes to near normal levels (Fig. 4). In all instances, the observed improvements in MITO function parameters following treatment with elamipretide trended toward baseline (normal state) and at no time exceeded normal levels indicating that full recovery of MITO function was not necessary to achieve the degree of observed hemodynamic improvement. *In-Vitro* incubation of isolated cardiomyocytes from untreated HF dogs with increasing concentration of Elamipretide showed a concentration-dependent improvement in state-3 respiration. In the absence of elamipretide, ADP-stimulated respiration was 248±9 nAtom O/min/mg protein and increased to 303±33 at 0.01 μM, 405±39 at 0.1 μM and to 371±28 at 1.0 μM concentration of elamipretide.

Proteins that Modulate Mitochondrial Function—There were no differences in protein level of the internal control β-actin between normal dogs (0.44 ± 0.05 du) and HF-CON (0.41 ± 0.04 du) or elamipretide-treated HF dogs (0.45 ± 0.04 du). Proteins that regulate MITO biogenesis and respiration were dysregulated in HF-CON compared to normal dogs (Fig. 5). Compared to normal, levels of eNOS and PGC-1α were significantly decreased in HF-CON whereas iNOS was significantly up-regulated. Elamipretide normalized levels of both NOS isoforms and PGC-1α (Fig. 5). Cytosolic levels of cytochrome c were significantly increased in HF-CON as were tissue levels of active caspase-3. Treatment with elamipretide normalized the expression of both pro-apoptotic proteins (Fig. 5). Compared to normal, HF-CON dogs had significantly lower levels of SERCA-2a which was significantly increased to near normal by elamipretide (Fig. 5). Total CL and total CL normalized to MITO protein were significantly decreased in LV of HF-CON compared to normal dogs as were the levels of total $(18:2)_4$CL subspecies and total $(18:2)_4$CL subspecies normalized to MITO protein. Treatment with elamipretide significantly increased all measures to near normal levels (Fig. 6). Protein levels of key subunits of MITO complexes I-V decreased significantly in HF dogs compared to normal dogs (Fig. 7, Table 4). Treatment with elamipretide partially restored normal levels of all

key subunits. Compared to untreated controls, levels of subunits of complexes I, II and IV improved significantly after long-term therapy with elamipretide whereas the observed improvement in subunits of complexes III and V did not reach statistical significance (Fig. 7, Table 4). In all instances, the observed improvements in protein levels following treatment with elamipretide trended toward baseline (normal state) and at no time exceeded normal levels.

Discussion

The results indicate that long-term monotherapy with elamipretide improves LV function and prevents progressive LV enlargement. The magnitude of improvement is similar to that observed in this canine HF model after long-term therapy with ACE inhibitors and beta-blockers (27). Improved LV function was associated with reductions in plasma biomarkers of natriuretic peptides and pro-inflammatory cytokines and was not associated with significant changes in HR, mAoP or SVR. These benefits occurred alongside normalization of MITO function evidenced by improved rate of ATP synthesis and reduced ROS formation. Elamipretide also attenuated structural LV remodeling evidenced by reduction of cardiomyocyte hypertrophy and interstitial fibrosis and increased capillary density (23, 24, 28). Normalization of these structural components likely promotes greater LV compliance and tissue oxygenation and hence improved passive LV filling and overall LV function. The improvements in histomorphometric measure of structural remodelling after treatment with elamipretide are similar in magnitude to those seen in this canine HF model after monotherapy with AT1 receptor antagonists and beta-blockers (29, 30).

In this study, chronic treatment with elamipretide improved energy availability in the failing myocardium evidenced by increased maximum rate of ATP synthesis and increased ATP/ADP ratio. In addition to improving MITO state-3 respiration, MITO membrane potential and reducing opening of the mPTP, treatment with elamipretide also normalized the activity of complex-I and complex-IV while limiting the formation of ROS. Improved ATP synthesis by mitochondria can also lead to improved sarcoplasmic reticulum calcium cycling by increasing Ca^{2+}-ATPase (SERCA-2a) activity. Reduced SERCA-2a activity and expression are key maladaptations in HF. Treatment with elamipretide was associated with improved protein levels of SERCA-2a.

The improvement in MITO function following long-term therapy with elamipretide leads to normalization of CL. The latter is likely facilitated by the ability of elamipretide to permeate the outer MITO membrane and bind to CL, a signature phospholipid of the inner MITO membrane that plays an important role in cristae formation, activity of respiratory complexes, organization of the respiratory complexes into supercomplexes for oxidative phosphorylation, MITO fusion and MITO DNA stability and segregation (10–12, 14,31). CL is biosynthesized in a series of steps from phosphatidic acid and remodeled into a form which contains four 18:2 fatty acid chains, tetralinoleol CL [$(18:2)_4$CL]. Cardiolipin peroxidation and depletion have been reported in a variety of pathological conditions associated with energy deficiency (14). In the present study, total CL and $(18:2)_4$CL were decreased in LV myocardium of dogs with HF and treatment with elamipretide normalized total CL and $(18:2)_4$CL. The decrease in CL was driven by changes in the lipid structure on

the inner MITO membrane due to peroxidation and not necessarily a reflection of changes in the total LV myocardial pool of MITO protein. This observation is also supported by results showing concordant changes in LV myocardial levels of 4-HNE, a major product of lipid peroxidation. Nevertheless, additive beneficial effects of elamipretide on mitochondrial biogenesis/turnover may also co-exist alongside membrane remodeling. CL is essential for activity of MITO complexes and, in particular complex I and complex-IV. Defects of complex I are integral to the formation of ROS whereas complex-IV is essential for oxidative phosphorylation. In the present study, elamipretide normalized the activity of complex-I and IV, a finding consistent with normalization of CL. Elamipretide also restored, albeit in part, levels of key subunits of MITO complexes I through V and reduced the formation of ROS in LV myocardium. Preserving CL is also important in respiratory function through supercomplex assembly. Even though supercomplex expression was not measured in the present study, others have shown that elamipretide preserves supercomplex-dependent MITO function in LV myocardium of rats subjected to ischemia-reperfusion injury (32).

Even though the primary objective of this study was to evaluate the chronic effects of elamipretide, we also showed that a short-term (2 hours) intravenous infusion of elamipretide improved LV systolic function and that *in-vitro* incubation of failing canine cardiomyocytes in increasing concentration of elamipretide elicits improvement in ADP-dependent (state-3) MITO respiration. These results indicate that elamipretide can elicit short-term benefits on LV function possibly through improved MITO function as evidence by improved respiration. The data also suggest that an improvement in the abundance of 18:2 CL is not required in the short-term for enhancement of MITO function by elamipretide. It is not likely that novel synthesis and remodeling of CL can occur in a short 2 hour span of elamipretide infusion. It is possible, although remains to be shown, that the electrostatic interaction between elamipretide and CL is itself sufficient to stabilize the complexes on the electron transport chain (ETC) and, in doing so, improve efficiency of the electron transfer culminating in reduced ROS and enhanced oxidative phosphorylation. This explanation is supported by studies of old mice with MITO dysfunction (33) in which resting and maximal MITO ATP production and cell energy state (phosphocreatine/ATP) were rapidly reversed only one hour after injection of elamipretide (33).

Mitochondria are a major source of ROS production. Excess ROS formation can lead to tissue injury, cardiomyocyte degeneration and programmed cell death. Increased ROS can contribute to increase opening of the mPTP (34) and has been shown to interact with calcium signaling and several ion channels involved in cardiac hypertrophy signaling and its progression to HF (35, 36). We previously showed that HF is associated with opening of the mPTP with an attendant increase in the level of cytochrome c in the cytosol and consequently an increase in cardiomyocyte apoptosis (7, 8, 37). In the present study, long-term therapy with elamipretide reduced ROS formation, attenuated mPTP openings and significantly decreased the levels of cytosolic cytochrome c and active caspase-3 thus suppressing a major signaling pathway for apoptosis. Levels of plasma pro-inflammatory cytokines were reduced in the present study following chronic treatment with elamipretide. We are not aware of any evidence that elamipretide acts directly as an anti-inflammatory. It

is more likely that by reducing excessive ROS formation, elamipretide limits tissue injury and, in doing so, attenuates pro-inflammatory cytokines.

In conclusion, this is the first study to our knowledge where the effects of long-term therapy with elamipretide were evaluated in a chronic model of HF. The results support the hypothesis that targeting MITO dysfunction in HF is key to improving overall LV function. Elamipretide represents a new class of compounds that can improve the availability of energy to failing heart and reduce the burden of tissue injury caused by excessive ROS production. In doing so, elamipretide limits end-organ damage and ensures the production of energy commensurate with the needs of the myocardium for improving cell function and overall LV performance.

Supplementary Material

Refer to Web version on PubMed Central for supplementary material.

Acknowledgments

Sources of Funding

This study was supported, in part, by a research grant from Stealth Biotherapeutics, Inc. and by National Heart, Lung, and Blood Institute PO1 HL074237-10.

References

1. Marcinek D, Schenkman KA, Ciesielski W, Lee D, Conley K. Reduced mitochondrial coupling in vivo alters cellular energetics in aged mouse skeletal muscle. J Physiol. 2005; 569:467–473. [PubMed: 16254011]
2. Brown DA, Sabbah HN, Shaikh. Mitochondrial inner membrane lipids and proteins as targets for decreasing cardiac ischemia/reperfusion injury. Pharmacology & Therapeutics. 2013; 140:258–266. [PubMed: 23867906]
3. Kloner RA, Hale SL, Dai W, Gorman RC, Shuto T, Koomalsingh KJ, Gorman JH, Sloan RC, Frasier CR, Watson CA, Bostian PA, Kypson AP, Brown DA. Reduction of ischemia/reperfusion injury with Bendavia, a mitochondria-targeting cytoprotective peptide. J Am Heart Assoc. 2012; 1:1–13. [PubMed: 23130111]
4. Eirin, Alfonso; Li, Zilun; Zhang, Xin; Krier, James D.; Woollard, John R.; Zhu, Xiang-Yang; Tang, Hui; Herrmann, Sandra M.; Lerman, Amir; Textor, Stephen C.; Lerman, Lilach O. A Mitochondrial permeability transition pore inhibitor improves renal outcomes after revascularization in experimental atherosclerotic renal artery stenosis. Hypertension. 2013; 60:1242–1249. [PubMed: 23045468]
5. Sabbah HN, Sharov V, Riddle JM, Kono T, Lesch M, Goldstein S. Mitochondrial abnormalities in myocardium of dogs with chronic heart failure. J Mol Cell Cardiol. 1992; 11:1333–1347. [PubMed: 1479624]
6. Sharov VG, Goussev A, Lesch M, Goldstein S, Sabbah HN. Abnormal mitochondrial function in myocardium of dogs with chronic heart failure. J Mol Cell Cardiol. 1998; 30:1757–1762. [PubMed: 9769231]
7. Sharov VG, Todor A, Khanal S, Imai M, Sabbah HN. Cyclosporine A attenuates mitochondrial permeability transition and improves mitochondrial respiratory function in cardiomyocytes isolated from dogs with heart failure. J Mol Cell Cardiol. 2007; 42:150–158. [PubMed: 17070837]
8. Sharov VG, Todor AV, Silverman N, Goldstein S, Sabbah HN. Abnormal mitochondrial respiration in failed human myocardium. J Mol Cell Cardiol. 2000; 32:2361–2367. [PubMed: 11113011]

9. Zhao K, Luo G, Zhao GM, Schiller PW, Szeto HH. Transcellular transport of a highly polar 3^{+} net charge opioid tetrapeptide. The Journal of pharmacology and experimental therapeutics. 2003; 304:425–432. [PubMed: 12490619]
10. DeVay RM, Dominguez-Ramirez L, Lackner LL, Hoppins S, Stahlberg H, Nunnari J. Coassembly of Mgm1 isoforms requires cardiolipin and mediates mitochondrial inner memberane fusion. J Cell Biol. 2009; 186:793–803. [PubMed: 19752025]
11. Joshi AS, Thompson MN, Fei N, Huttermann M, Greenberg ML. Cardiolipin and mitochondrial phosphatidylethanolamine have overlapping functions in mitochondrial fusion in Saccharomyces cerevisiae. J Biol Chem. 2012; 287:17589–17597. [PubMed: 22433850]
12. Luevano-Martinez LA, Forni MF, Tiago dios Santios V, Souza-Pinto NC, Kowaltowski AJ. Cardiolipin is a key determinant for mtDNA stability and segregation during mitochondrial stress. Biochimica et Biophysica Acta. 2015; 1847:587–598. [PubMed: 25843549]
13. Zhao K, Zhao GM, Wu D, Soong Y, Birk AV, Schiller PW, Szeto HH. Cell-permeable peptide antioxidants targeted to inner mitochondrial membrane inhibit mitochondrial swelling, oxidative cell death, and reperfusion injury. J Biol Chem. 2004; 279:34682–34690. [PubMed: 15178689]
14. Birk AV, Liu S, Soong Y, Mills W, Singh P, Warren JD, Seshan SV, Pardee JD, Szeto HH. The mitochondrial-targeted compound SS-31 re-energizes ischemic mitochondria by interacting with cardiolipin. J Am Soc Nephrol: JASN. 2013; 24:1250–1261. [PubMed: 23813215]
15. Dai DF, Hsieh EJ, Chen T, Menendez LG, Basisty NB, Tsai L, Beyer RP, Crispin DA, Shulman NJ, Szeto HH, Tian R, MacCoss MJ, Rabinovitch PS. Global proteomics and pathway analysis of pressure-overload-induced heart failure and its attenuation by mitochondrial-targeted peptides. Circ-Heart Fail. 2013; 6:1067–1076. [PubMed: 23935006]
16. Szeto HH, Liu S, Soong Y, Wu D, Darrah SF, Cheng FY, Zhao Z, Ganger M, Tow CY, Seshan SV. Mitochondria-targeted peptide accelerates ATP recovery and reduces ischemic kidney injury. J Am Soc Nephr: JASN. 2011; 22:1041–1052.
17. Talbert EE, Smuder AJ, Min K, Kwon OS, Szeto HH, Powers SK. Immobilization-induced activation of key proteolytic systems in skeletal muscles is prevented by a mitochondria-targeted antioxidant. J Appl Physiol. 2013; 115:529–538. [PubMed: 23766499]
18. Yang L, Zhao K, Calingasan NY, Luo G, Szeto HH, Beal MF. Mitochondria targeted peptides protect against 1-methyl-4-phenyl-1,2,3,6-tetrahydropyridine neurotoxicity. Antioxidants & Redox Signaling. 2009; 11:2095–2104. [PubMed: 19203217]
19. Brown DA, Hale SL, Baines CP, Rio CL, Hamlin RL, Yueyama Y, Kijtawornrat A, Yeh ST, Frasier CR, Stewart LM, Moukdar F, Shaikh SR, Fisher-Wellman KH, Neufer PD, Kloner RA. Reduction of early reperfusion injury with the mitochondria-targeting peptide Bendavia. J Cardiovasc Pharmacol Ther. 2014; 19:121–132. [PubMed: 24288396]
20. Sabbah HN, Stein PD, Kono T, Gheorghiade M, Levine TB, Jafri S, Hawkins ET, Goldstein S. A canine model of chronic heart failure produced by multiple sequential coronary microembolizations. Am J Physiol. 1991; 260:H1379–H1384. [PubMed: 1826414]
21. Bonow RO. New insights into the cardiac natriuretic peptides. Circulation. 1996; 93:1946–1950. [PubMed: 8640966]
22. Kobayashi, Hiroshi; Gil-Guzman, Enrique; Mahran, Ayman M.; Sharma, Rakesh K.; Nelson, David R.; Thomas, Anthony J., Jr; Agarwal, Askok. Quality Control of Reactive Oxygen Species Measurement by Luminol-Dependent Chemiluminescence Assay. Journal of Andrology. 2001; 22:568–574. [PubMed: 11451353]
23. Liu YH, Yang XP, Sharov VG, Nass O, Sabbah HN, Peterson E, Carretero OA. Effects of angiotensin-converting enzyme inhibitors and angiotensin II type 1 receptor antagonists in rats with heart failure. Role of kinins and angiotensin II type 2 receptors. J Clin Invest. 1997; 99:1926–1935. [PubMed: 9109437]
24. Sabbah HN, Stanley WC, Sharov VG, Mishima T, Tanimura M, Benedict CR, Hegde S, Goldstein S. Effects of dopamine beta-hydroxylase inhibition with nepicastat on the progression of left ventricular dysfunction and remodeling in dogs with chronic heart failure. Circulation. 2000; 102:1990–1995. [PubMed: 11034950]

25. O'Toole JF, Patel HV, Naples CJ, Fujioka H, Hoppel CL. Decreased cytochrome c mediates an age-related decline of oxidative phosphorylation in rat kidney mitochondria. Biochem J. 2010; 427:105–112. [PubMed: 20100174]
26. He Q, Han X. Cardiolipin remodeling in diabetic heart. Chem Phys Lipids. 2014; 179:75–81. [PubMed: 24189589]
27. Sabbah HN, Shimoyama H, Kono T, Gupta RS, Sharov VG, Scicli G, Levine TB, Goldstein S. Effects of long-term monotherapy with enalapril, metoprolol and digoxin on the progression of left ventricular dysfunction and dilation in dogs with reduced ejection fraction. Circulation. 1994; 89:2852–2859. [PubMed: 8205701]
28. Sabbah HN, Sharov VG, Lesch M, Goldstein S. Progression of heart failure: A role for interstitial fibrosis. Mol Cell Biochem. 1995; 147:29–34. [PubMed: 7494551]
29. Tanimura M, Sharov VG, Shimoyama H, Mishima T, Levine TB, Goldstein S, Sabbah HN. Effects of AT_1 receptor blockade on the progression of left ventricular dysfunction in dogs with heart failure. Am J Physiol. 1999; 276:H1385–H1392. [PubMed: 10199866]
30. Zaca V, Rastogi S, Mishra S, Imai M, Wang M, Gupta RC, Jiang A, Sharov VG, Goldstein S, Sabbah HN. Atenolol is inferior to metoprolol in improving left ventricular function and preventing ventricular remodeling in dogs with heart failure. Cardiology. 2009; 112:294–302. [PubMed: 18832825]
31. Rosca MG, Vazquez EJ, Kerner J, Parland W, Chandler MP, Stanley WC, Sabbah HN, Hoppel CL. Cardiac mitochondria in heart failure: decrease in respirasomes and oxidative phosphorylation. Cardiovasc Res. 2008; 80:30–39. [PubMed: 18710878]
32. Brown DA, Moukdar F, Lark DS, Neufer PD, Shaikh SR. The cardiolipin-targeting peptide Bendavia preserves post-ischemic mitochondrial energetics by sustaining respiratory supercomplexes (Abst). Circ Res. 2014; 115:A337.
33. Siegel MP, Kruse SE, Percival JM, Goh J, White CC, Hopkins HC, Kavanagh TJ, Szeto HH, Rabinovitch PS, Marcinek DJ. Mitochondrial-targeted peptide rapidly improves mitochondrial energetics and skeletal muscle performance in aged mice. Aging Cell. 2013; 12:763–771. [PubMed: 23692570]
34. Halestrap AP, Pasdois P. The role of the mitochondrial permeability transition pore in heart disease. Biochimica et biophysica acta. 2009; 1787:1402–15. [PubMed: 19168026]
35. Burgoyne JR, Mongue-Din H, Eaton P, Shah AM. Redox signaling in cardiac physiology and pathology. Circulation research. 2012; 111:1091–106. [PubMed: 23023511]
36. Dai DF, Rabinovitch PS, Ungvari Z. Mitochondria and cardiovascular aging. Circulation research. 2012; 110:1109–24. [PubMed: 22499901]
37. Sharov VG, Sabbah HN, Shimoyama H, Goussev AV, Lesch M, Goldstein S. Evidence of cardiocyte apoptosis in myocardium of dogs with chronic heart failure. The American journal of pathology. 1996; 148:141–9. [PubMed: 8546201]

Clinical Perspective

Structural and functional abnormalities exist in constituent mitochondria of the failing heart and can lead to excessive production of reactive oxygen species (ROS) and, importantly, to reduced rate of ATP synthesis, the energy currency of living cells and the lifeline of cardiomyocytes. Excessive formation of ROS results in tissue injury while reduced rate of ATP synthesis contributes to cellular dysfunction with both contributing to progressive worsening of left ventricular (LV) function that characterizes the heart failure (HF) state. The absence of drugs that can prevent, reverse or even limit mitochondrial dysfunction in HF has contributed to the lack of research exploring the potential therapeutic merits of reversing mitochondrial dysfunction in HF. Current HF drugs elicit their benefits largely by reducing cardiac workload that leads to reduced myocardial energy demands to levels in-line with the existing limited energy supply. This pre-clinical study in dogs with chronic HF describes the effects of a novel, first in class mitochondria targeting peptide, elamipretide, that normalizes many of the abnormalities of mitochondria in HF. Elamipretide improved LV function, prevented progressive LV remodeling and normalized plasma biomarkers. These improvements were associated with normalization of mitochondrial function evidenced by normalization of mitochondrial respiration, membrane potential, complex activities and rate of ATP synthesis along with reduction in ROS formation. If these pre-clinical observations translate into the clinic and elamipretide shows benefits in HF patients, this approach will likely usher in a new HF therapeutic paradigm; one that is based on providing needed energy supply to meet increased cardiac demands and one that is likely to be additive to “standard of care” therapies.

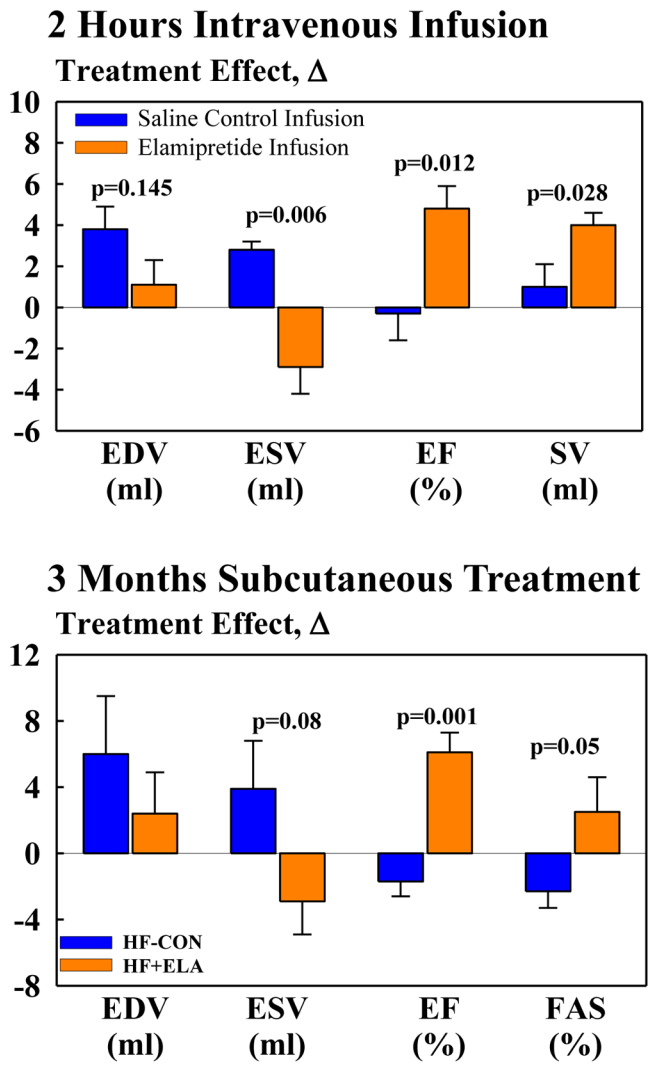

Figure 1.

Top: Change Δ (treatment effect) between pre-treatment and 2 hour intravenous infusion of elamipretide on left ventricular (LV) end-diastolic volume (EDV), end-systolic volume (ESV), ejection fraction (EF) and stroke volume (SV) in untreated heart failure control dogs (HF-CON) and heart failure dogs treated with elamipretide (HF+ELA). Bottom: Change Δ (treatment effect) between pre-treatment and 12 weeks post-treatment for LV EDV, ESV, EF and fractional area of shortening (FAS) in HF-CON and HF+ELA dogs. Probability values are comparisons between HF-CON and HF+ELA dogs. Statistical significance based on t-statistic for two means. All bar graphs are depicted as Mean±SEM.

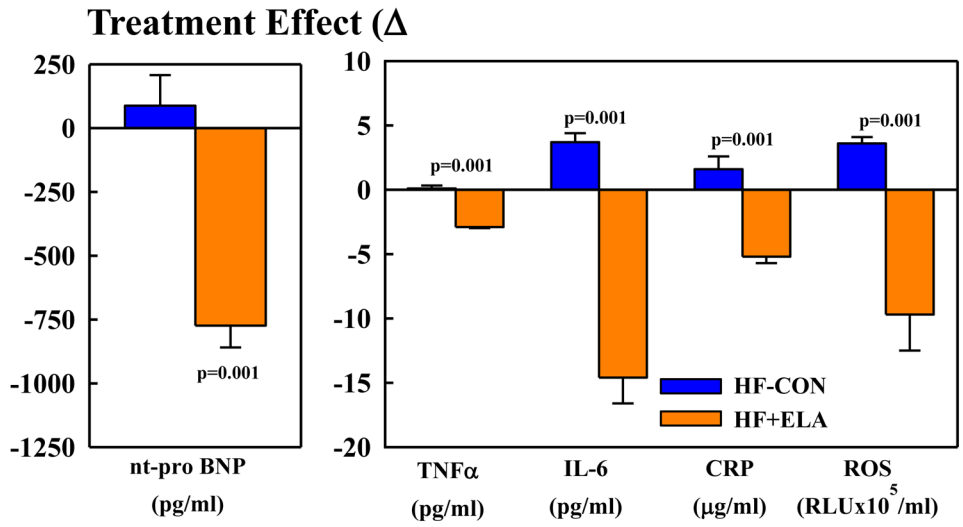

Figure 2.

Change Δ (treatment effect) between pre-treatment and 12 weeks post-treatment for plasma levels of n-terminal pro-brain natriuretic peptide (nt-pro BNP), tumor necrosis factor-α (TNF-α), interleukin-6 (IL-6), c-reactive protein (CRP) and reactive oxygen species (ROS). Probability values are comparisons between heart failure control dogs (HF-CON) and elamipretide-treated heart failure dogs (HF+ELA). Statistical significance based on t-statistic for two means. All bar graphs are depicted as Mean±SEM.

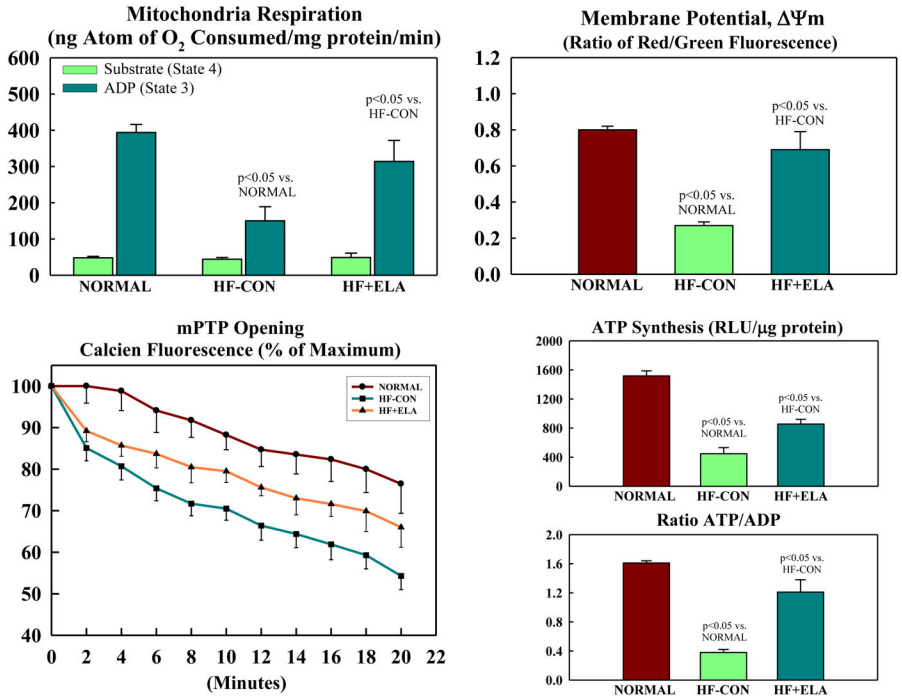

Figure 3.

Mitochondrial function in cardiomyocytes of left ventricular myocardium of normal dogs, untreated heart failure control dogs (HF-CON) and dogs with heart failure treated with elamipretide (HF+ELA). Top Left: Mitochondrial state 3 and 4 respiration. Top Right: Mitochondrial membrane potential. Bottom Left: Mitochondrial permeability transition pore (mPTP). Bottom Right: Maximum rate of adenosine triphosphate (ATP) synthesis and ratio of ATP to adenosine diphosphate (ADP). Probability values are comparisons between normal dogs, HF-CON and HF-ELA dogs. Statistical significance based on one way ANOVA followed by the Student-Neuman-Keuls. All bar graphs are depicted as Mean ±SEM.

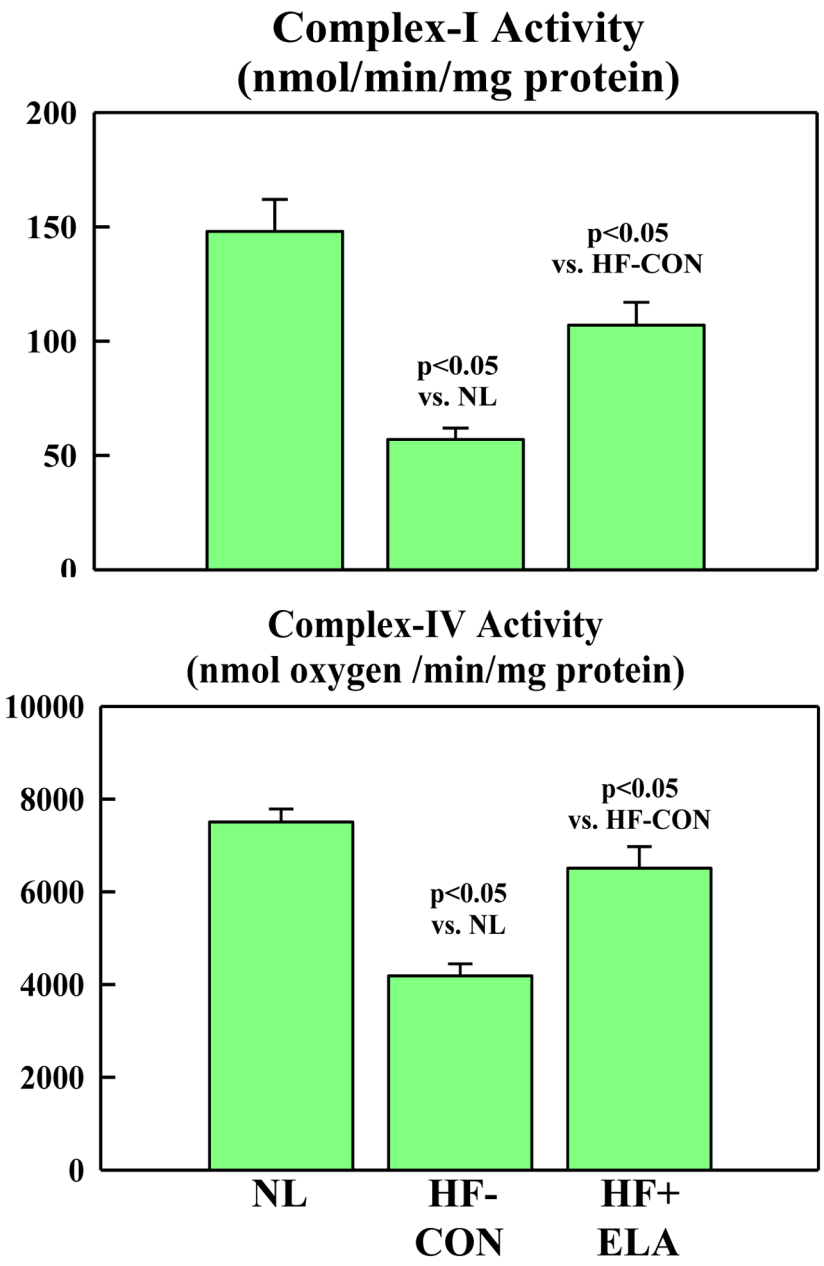

Figure 4.

Bar graphs (Mean±SEM) depicting Complex-I (Top) and Complex-IV (Bottom) enzymatic activity in LV myocardium of normal (NL) dogs, untreated heart failure control dogs (HF-CON) and dogs with heart failure treated with elamipretide (HF+ELA). Statistical significance based on one way ANOVA followed by the Student-Neuman-Keuls.

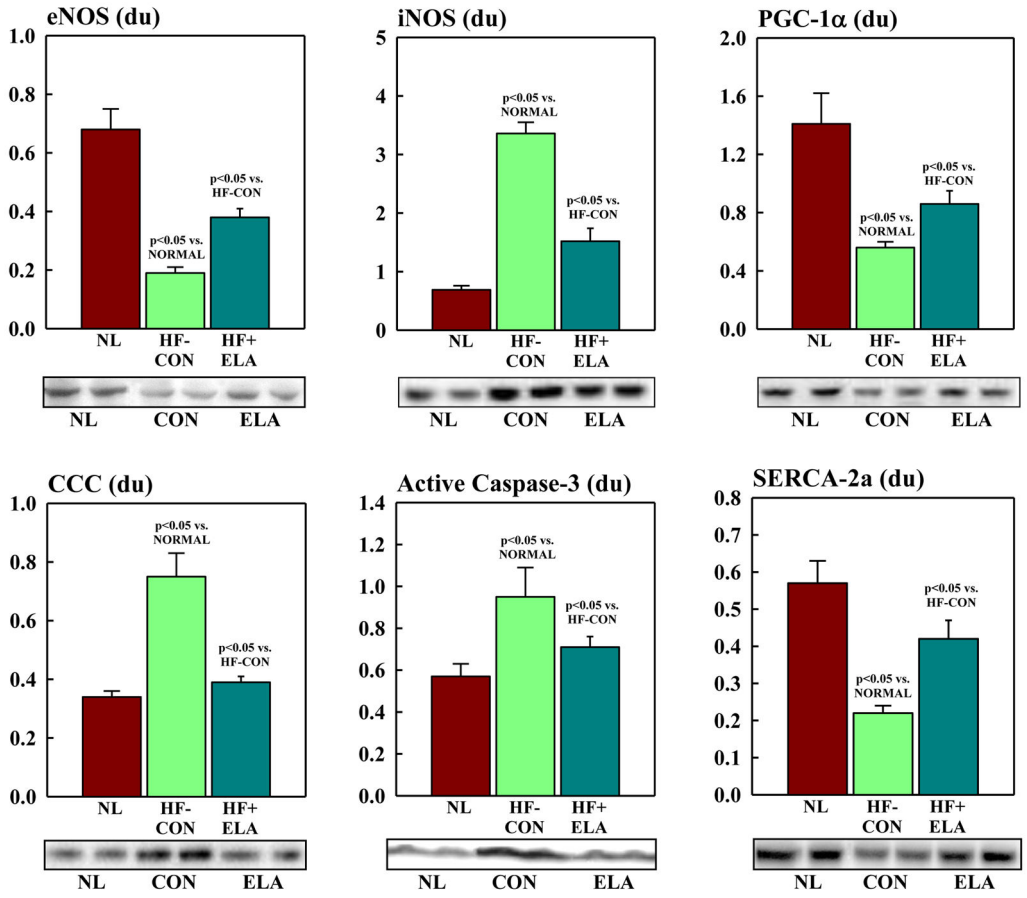

Figure 5.

Bar graphs (Mean±SEM) depicting protein levels of endothelial nitric oxide synthase (eNOS), inducible nitric oxide synthase (iNOS), peroxisome proliferator-activated receptor coactivator-1α (PGC-1α), cytosolic cytochrome c, active caspase 3 and sarcoplasmic reticulum (SR) Ca^{2+}-ATPase (SERCA-2a) in LV myocardium of normal dogs (NL), untreated ailure control dogs (HF-CON) and heart failure dogs treated with elamipretide (HF+ELA). Below each graph, are bands from Western Blots of each protein. du=densitometric units. Statistical significance based on one way ANOVA followed by the Student-Neuman-Keuls.

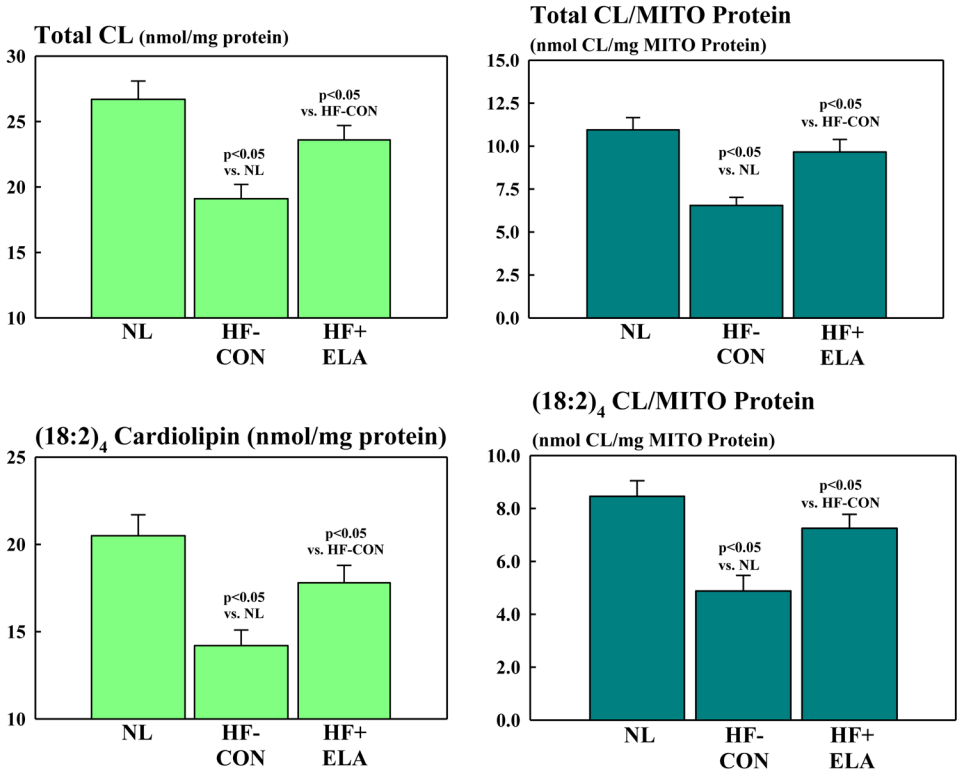

Figure 6.

Bar graphs (Mean±SEM) depicting total cardiolipin (CL) level (Top Left) and total cardiolipin level normalized to mitochondrial (MITO) protein (Top Right and total $(18:2)_4$ cardiolipin level (Bottom Left) and total $(18:2)_4$ cardiolipin level normalized to mitochondrial protein level (Bottom Right) in LV myocardium of normal (NL) dogs, untreated heart failure control dogs (HF-CON) and dogs with heart failure treated with elamipretide (HF+ELA). Statistical significance based on one way ANOVA followed by the Student-Neuman-Keuls.

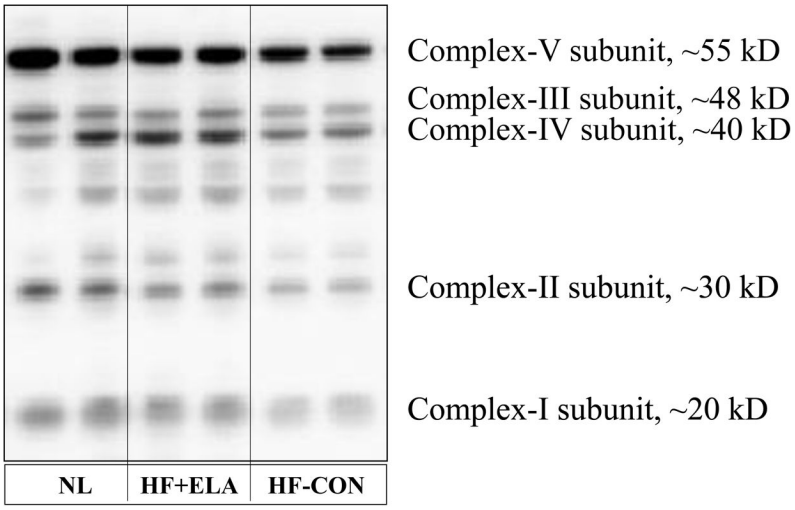

Figure 7.

Western blots of protein abundances of key mitochondrial subunits of mitochondrial complexes I, II, III, IV and V performed using Total OXPHOS Western Blot Antibody Cocktail ab110413. The blot depicts results from 2 normal dogs (NL), 2 untreated heart failure control dogs (HF-CON) and 2 dogs with heart failure treated with elamipretide (HF +ELA). The specific subunits are listed in the Methods section.

TABLE 1

Hemodynamic, ventriculographic, echocardiographic and plasma biomarker measures in untreated heart failure control dogs (HF-CON) (n=7) and heart failure dogs treated with elamipretide (HF+ELA) (n=7).

	HF-CON			HF+ELA		
	Baseline	**Pre-treatment**	**Post-treatment**	**Baseline**	**Pre-treatment**	**Post-treatment**
Body Weight (kg)	22.7±0.7	23.1±0.7	24.0±0.5	21.5±0.4	22.1±0.4	23.0±0.7
HR (beats/min)	86±2	88±2	84±1	90±3	82±2*	84±3
mAoP (mmHg)	72±1	74±1	74±1	75±1	73±2	71±1
LVEDP (mmHg)	12±1	15±1*	16±1*	12±1	17±1*	14±0.3*†
LVEDV (ml)	57±3	63±3	69±5*	62±2	75±4*	77±3*
LVESV (ml)	28±1	44±3*	48±4*	32±1	52±2*	49±2*
LVEF (%)	51±1	31±1*	29±1*	49±1	30±2*	36±2*†
SV (ml)	29±2	19±1*	21±2*	31±1	23±2*	28±2†
CO (L/min)	2.5±0.16	1.7±0.11*	1.76±0.15*	2.73±0.08	1.86±0.14*	2.34±0.11*†
CI (L/min/m^2)	3.2±0.2	2.1±0.1*	2.1±0.2*	3.3±0.1	2.2±0.2*	2.8±0.1*†
SVR (dynes-sec-cm^{-5})	2809±156	4223±232*	3855±274*	2642±105	3647±326*	2916±167†
Ei/Ai	7.5±0.9	4.5±0.4*	4.2±0.3*	7.3±1.0	4.8±0.6*	5.3±0.6*
DT (msec)	102±2	79±4*	73±5*	102±4	75±5*	84±4*
LV EDWS (gm/cm^2)	46±2	77±3*	78±9*	47±3	87±9*	69±7*†
nt-Pro BNP (pg/ml)	262±15	1163±126*	1250±113*	278±17	1128±72*	354±29*†
TNF-α (pg/ml)	1.29±0.14	3.85±0.16*	3.95±0.23*	1.24±0.13	4.36±0.09*	1.44±0.09†
IL-6 (pg/ml)	9.1±2.3	24.9±2.1*	28.6±1.9*†	10.1±1.1	26.6±2.2*	12.0±0.3*†
CRP (μg/ml)	1.30±0.16	7.38±0.65*	8.99±1.36*	1.69±0.19	6.89±0.70*	1.72±0.29†
Plasma ROS (RLUx10^5/ml)	5.0±0.3	21.1±3.1*	23.8±2.0*	5.3±0.5	20.7±2.6*	10.5±0.8*†

HR=heart rate; mAoP=mean aortic pressure; LV=left ventricular; EDP=end-diastolic pressure; EDV=end-diastolic volume; ESV=end-systolic volume; EF=ejection fraction; SV=stroke volume; CO=cardiac output; CI=cardiac index; SVR=systemic vascular resistance; Ei=time-velocity integral of the mitral inflow velocity waveform representing early filling; Ai= time-velocity integral representing left atrial contraction; Ei/Ai=ratio of Ei to Ai; DT=deceleration time of early mitral inflow velocity; EDWS=LV end-diastolic circumferential wall stress; nt-Pro-BNP=n-terminal-pro brain natriuretic peptide; TNF-α=tumor necrosis factor alpha; IL=interleukin; CRP=C-reactive protein; ROS = level of reactive oxygen species in plasma; RLU = relative light units. All data are Mean±SEM.

* p<0.05 vs. baseline;

† p<0.05 vs. pre-treatment

Table 2

Treatment effect (Δ) in untreated heart failure control dogs (HF-CON) (n=7) and in elamipretide-treated heart failure dogs (HF+ELA) (n=7).

	HF-CON	HF+ELA	P-value
Δ Body weight (kg)	0.8±0.5	0.9±0.3	0.87
Δ HR (beats/min)	−3.7±2.1	1.7±2.3	0.11
Δ mAoP (mmHg)	0.1±1.6	−1.3±1.6	0.54
Δ LVEDP (mmHg)	0.6±0.6	−2.3±0.5	0.003
Δ SV (ml)	2.1±1.5	5.3±1.2	0.13
Δ CO (L/min)	0.10±0.14	0.48±0.14	0.05
Δ CI (L/m^2)	0.1±0.2	0.6±0.1	0.05
Δ SVR (dynes-sec-cm^{-5})	−367±285	−781±228	0.28
Δ Ei/Ai	−0.3±0.2	0.4±0.7	0.36
Δ DT (msec)	−5.7±6.5	8.4±5.1	0.11
Δ EDWS (gm/cm^2)	0.9±9.0	−17.6±3.4	0.08

Abbreviations as in Table 1. All data are Mean±SEM. P-value=probability value between HF-CON and HF+ELA. Values less than 0.05 are considered significant.

Table 3

Histomorphometric findings at the end of 3 months in normal dogs (n=7), in untreated heart failure control dogs (HF-CON) (n=7) and in heart failure dogs treated with elamipretide (HF+ELA) (n=7).

	VFRF (%)	VFIF (%)	CD (cap/mm^2)	ODD (μm)	MCSA (μm^2)
Normal	0.0	3.7±0.07	2609±79.5	8.9±0.17	410±10.0
HF-CON	12.3±0.6*	11.8±0.5*	1806±80*	12.6±0.2*	678±5.4*
HF+ELA	11.2±0.9	9.7±0.5†	2026±127†	11.4±0.4†	600±4.3†

Data are shown as Mean ± SEM. VFIF=volume fraction of interstitial fibrosis; VFRF=volume fraction of replacement fibrosis; CD=capillary density; ODD=oxygen diffusion distance; MCSA=myocyte cross-sectional area. All data are Mean±SEM.

*p<0.05 vs. Normal,

†p<0.05 vs. HF-CON.

Table 4

ROS and 4-HNE levels and MITO complexes I, II, III, IV, and V abundances in LV myocardium of normal dogs (n=6), untreated heart failure control dogs (HF-CON) (n=7) and elamipretide-treated heart failure dogs (HF+ELA) (n=7).

	Normal	HF-CON	HF+ELA
LV Tissue ROS (RLUx10^4/μg protein)	0.77±0.04	1.45±0.18*	0.90±0.06*†
4-HNE adducts (ng/mg protein)	185±21	399±35*	252±18*†
Complex-I subunit (du)	0.51±0.02	0.15±0.01*	0.29±0.03*†
Complex-II subunit (du)	0.45±0.06	0.14±0.01*	0.34±0.02*†
Complex-III subunit (du)	0.40±0.07	0.16±0.02*	0.27±0.03*
Complex-IV subunit (du)	0.61±0.04	0.26±0.05*	0.44±0.03*†
Complex-V subunit (du)	4.97±0.32	2.12±0.37*	2.81±0.50*

ROS=reactive oxygen species; 4-HNE=4-hydroxynonenal. All data are Mean±SEM.

* $p<0.05$ vs. Normal;

† $p<0.05$ vs. HF-CON.